

Searching for White Dwarf Exoplanets: WD 2359-434 Case Study

Bruce L. Gary
5320 E. Calle Manzana, Hereford, AZ 85615
BLGary@umich.edu

T. G. Tan
115 Adelma Rd., Dalkeith, WA 6009, Australia
tgtan@bigpond.net.au

Ivan Curtis
2 Yandra St., Vale Park, Adelaide, Australia
Ivan.Curtis@Keywords.com.au

Paul J. Tristram
Mt. John University Observatory
P.O.B. 56, Lake Tekapo 8770, New Zealand
Pjt61@ext.canterbury.ac.nz

Akihiko Fukui
Okayama Astrophysical Observatory, National Astronomical Observatory of Japan
3037-5 Honjo, Kamogata, Asakuchi, Okayama 719-0232, Japan
afukui@oao.nao.ac.jp

Abstract

The white dwarf WD 2359-434 was found to vary with a period of 2.695022 ± 0.000014 hours and semi-amplitude of 0.00480 ± 0.00023 magnitude. One explanation for the variation is a starspot with a 3.8-degree radius (assuming 500 K cooler than the surroundings) at latitude of ~ 27 degrees and a star rotation axis inclination of ~ 30 degrees. The brightness variation was very close to sinusoidal, and there were no changes in amplitude, period or phase during the 1.1 years of observations. This permitted consideration of an alternative explanation: a Jupiter-size exoplanet that reflects the white dwarf's light in amounts that vary with orbital position. Follow-up observations are suggested for distinguishing between these two interpretations.

1. Introduction

Photometric monitoring of 46 white dwarfs was conducted by 25 amateur observers located at a full range of longitudes during September, 2011 for the purpose of detecting transits produced by exoplanets. The observing project was called "Pro-Am White Dwarf Monitoring" (PAWM) and is described at the following web site: <http://brucegary.net/WDE/>. It was inspired by a publication by Agol (2011). No transit events of the expected shape were detected (~ 2 minutes length and > 0.1 magnitude fade), but two white dwarfs were found to be variable at the several milli-magnitude (mmag) level. Observations of one

of these variables continued past the PAWM observing month; it was observed again the following year from July to October. A total of 18 and 29 observing sessions, for 2011 and 2012, have been phase-folded and analyzed for the purpose of establishing constancy of the period, amplitude and phase. These data were also used for establishing the presence of any departure of the brightness variation shape from sinusoidal. The rationale for assessing the presence of amplitude or phase changes is that they could be accounted for by a starspot that varies in either size or location, and any such changes could be used to rule-out alternative explanations - such as the presence of an exoplanet reflecting light from the white dwarf (WD).

When a star is small, *e.g.*, $R_{\text{star}} \approx 0.9 \times R_{\text{Earth}}$, a Jupiter-size planet ($11 \times R_{\text{Earth}}$) is much larger than the star it orbits. Consequently, the light reflected by the planet can be a much greater fraction of the star’s light than if the star were a typical main sequence size. Also, a planet can orbit closer to a WD without tidal disruption than it could to a main sequence star; the closer a planet is to its star the brighter it’s reflected light will be. Therefore, if planets do orbit WDs it should be easier to detect their reflected light than it would be for a planet orbiting a main sequence star (Fossati *et al.*, 2012). Since many WDs don’t have spectra that allow accurate radial velocity (RV) measurements the RV method for detecting exoplanets won’t be as effective as the transit method. In fact, the RV method may not be as effective in searching for WD exoplanets as the reflected light method. WD 2359-434 can serve as illustration of this.

2. Previous Work

The number of known white dwarfs brighter than $V \approx 17$ is approximately 3000 (Agol and Relles, 2012). WD 2359-434 is a 13th magnitude star located at RA/DE = 00:02:11.34 -43:10:03.4 (J2000). It is spectral type DAP5.8 (exhibiting only hydrogen lines, magnetic with detected polarization). It has an estimated mass of $\sim 0.78 \times M_{\text{sun}}$ (Giammichelle *et al.*, 2012), $T_{\text{eff}} \sim 8,648$ K (Giammichelle *et al.*, 2012), and is located ~ 7.85 parsecs away (Holberg *et al.*, 2008). The H-alpha absorption line is sufficiently deep and narrow for the measurement of radial velocity (Maxted and Marsh, 1999). These authors report that the H-alpha line has “some hint of variability” in their 8 observations of WD 2359-434; their RV measurements rule out a companion WD because the RV range of ~ 10 km/s is ~ 15 times smaller than would be expected for a close binary. Dobbie *et al.* (2005) place an upper limit for any companion of $0.072 \times M_{\text{sun}}$ (*i.e.*, $< 75 \times M_{\text{Jupiter}}$), based on the absence of an infrared excess. This measurement also limits the amount of circumstellar dust that could be present close to WD 2359-434. The surface magnetic field is ~ 3.1 kG (Cuadrado *et al.*, 2004), which is considered low.

3. Observations

This paper reports observations made during the 2011 and 2012 observing seasons by four observatories, as summarized in the following table, showing telescope aperture, CCD camera, number of useable (and total taken) light curves observed and the observer’s amateur/professional status:

Observer	Telescope	CCD	LCs Useable (Total)	Amateur/Professional Status
Tan	12-inch	ST-8XME	32 (33)	Amateur
Curtis	11-inch	Atik 320	3 (4)	Amateur
Gary	14-inch	ST-10XME	1 (8)	Amateur
Tristram/Fukui	24-inch (B&C)	Apogee Alta U47	1 (2)	Professional

Table 1. Observer Information

Observatory locations are Perth, Australia (Tan), Adelaide, Australia (Curtis), Arizona (Gary) and Mt. John, New Zealand (Tristram/Fukui).

All-sky calibrations were conducted by author BLG on 2011.10.09 using the Hereford Arizona Observatory, consisting of a 14-inch fork-mounted Meade Schmidt-Cassegrain on an equatorial wedge. A 10-position filter wheel includes BVg’r’i’z’Cb filters. The CCD is a SBIG ST-10XME (KAF 3200E chip). The telescope is located in a dome, and all components are controlled from a control room via underground cables. Several Landolt star fields were used for establishing zero-shift and “star color sensitivity” parameters. The all-sky results are given in the following table.

B	V	r’	i’
13.278 ± 0.051	12.969 ± 0.039	12.949 ± 0.018	13.056 ± 0.022

Table 2. WD 2359-434 All-sky Magnitudes

For all observers images were calibrated (bias, dark and flat), star-aligned and processed with programs using a circular photometry aperture. Data files were sent to author BLG for subsequent analyses. A spreadsheet was used to produce a light curve (LC)

with the removal of “air mass curvature” (AMC). AMC is caused by atmospheric extinction that affects the target star (WD2359-434) differently from the average of the reference stars, due to atmospheric extinction’s monotonic increase with decreasing wavelength coupled with differences in the color of the target star and reference stars (i.e., red stars have a greater effective wavelength and lower extinction than blue stars). Since WD2359-434 is much bluer than all nearby stars the AMC correction changed LCs from the uncorrected “convex” shape to a flattened shape (with the 2.7-hour variation superimposed). This important step allowed for more accurate phase-folding of the many LCs made under different atmospheric extinction conditions.

Precision was determined for each LC by computing RMS noise based on internal consistency of magnitudes associated with each image; a running median of magnitudes from 4 images preceding and 4 images following served as reference for comparing single image magnitudes. Differences from this running median reference magnitude were used to identify outlier data. The number of images acquired per 10-minute interval was used to produce a value for “RMS per 10-minute interval” throughout the observing session. This was averaged for the interval when airmass < 2.0, and noted in a log of all LC data. The median “RMS per 10-minute interval” for LCs that were of sufficient quality to use for subsequent analysis was 1.9 mmag per 10-minute interval (R-band, N = 22) and 4.1 mmag (B-band, N = 8).

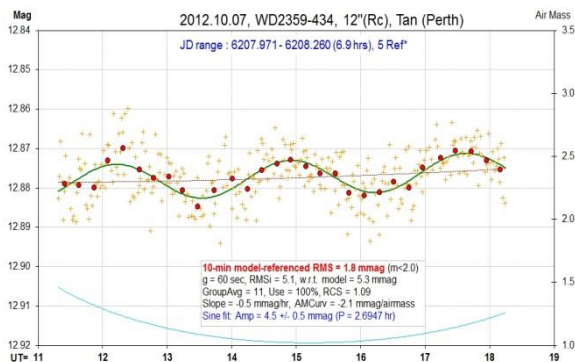


Figure 1. Typical light curve by author TGT.

The first evidence of variability was immediately obvious from the observation by author TGT on

2011.09.08. A period of ~ 2.7 hours was apparent, so it was possible for one observing session to sample as many as 3 complete periods. The semi-amplitude (later use of the term “amplitude” refers to semi-amplitude) was ~ 5 mmag, and is comparable to the single-image noise; since there are many images per period there is no ambiguity in fitting a sinusoidal function to the data. Figure 1 is a typical light curve by observer TGT (who provided 86% of useable LC observations).

Most observations were made with an Rc-band filter, but an effort was made to observe with a B-band filter (as well as V-, i'- and z'-band) for the purpose of assessing wavelength dependence of amplitude. None was found (discussed below), so this permitted all good quality light curves to be used in a phase-folding analysis. Since B, i' and z'-band data were noisier than for the other filter bands the phase-folding analysis included mostly Rc-band data.

4. Phase-Fold Fitting

Phase-folding was performed separately for the 2011 and 2012 observing seasons in order to assess the presence of changes in the three ephemeris parameters: period, amplitude and phase. These are shown as Figures 2 and 3. The period solutions for these two independent data sets are compatible, 2.694805 ± 0.00085 and 2.694926 ± 0.000073 hours (difference = 0.00012 ± 0.00011 hr). Projecting the (better determined) 2012 ephemeris to 2011 also yields phase agreement (BJDo difference = 17 ± 82 minutes). (Phase reference BJDo is defined using a sine function fitted to magnitude versus phase; brightness minimum therefore occurs at phase = 90 degrees.)

The 2011 and 2012 phase-folded data exhibit a small change in amplitude, from 5.52 ± 0.28 mmag to 4.64 ± 0.23 mmag. The amplitude difference is 0.88 ± 0.36 mmag (2.4-sigma), which appears to be statistically significant. The quoted uncertainties are based on a chi-squared analysis, which only includes stochastic sources of uncertainty (e.g., Poisson, thermal and scintillation). Systematic uncertainties can only be estimated, and they include AMC, slope

fitting, clock setting errors, and mistakes in converting JD to BJD, for example. If systematic uncertainties could be included in the chi-squared analysis the amplitude change would exhibit a greater uncertainty than the stated 0.36 mmag, and the 2.4-sigma significance would be reduced. We are therefore reluctant to claim that an amplitude change has been detected.

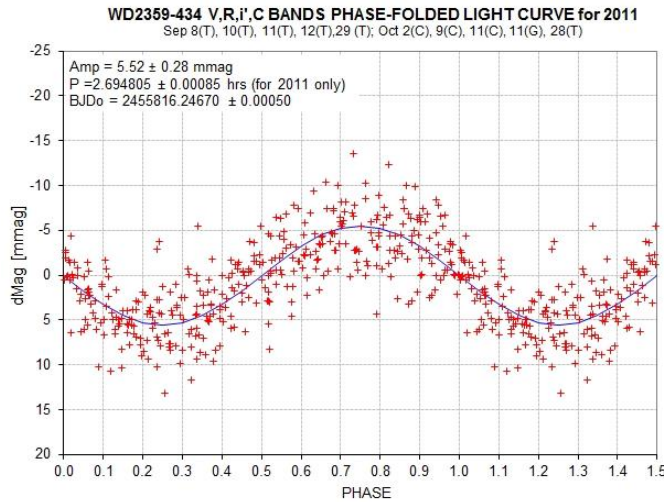


Figure 2. Phase-folded data from the 2011 observing season.

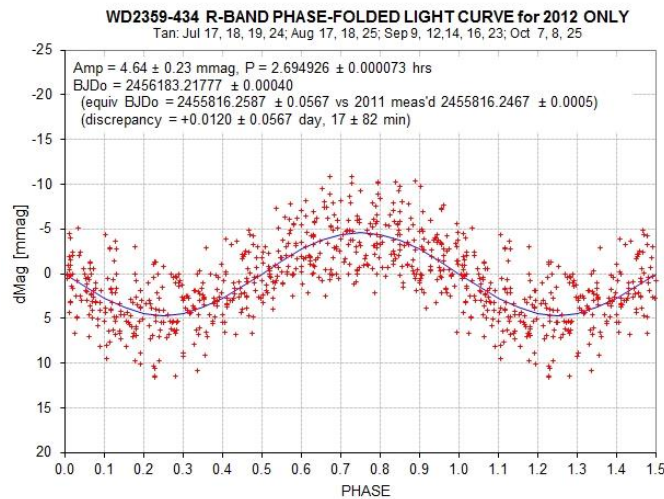


Figure 3. Phase-folded data for the 2012 observing season (TGT data only).

Given that between 2011 and 2012 there is no convincing evidence for a change in period, phase or amplitude, all data were combined to establish a more accurate ephemeris (period and phase), shown as Fig. 4. A phase-binned version of the same data is shown

as Fig. 5, which also includes a sinusoidal fit and starspot solution. The starspot solution is described in the next section.

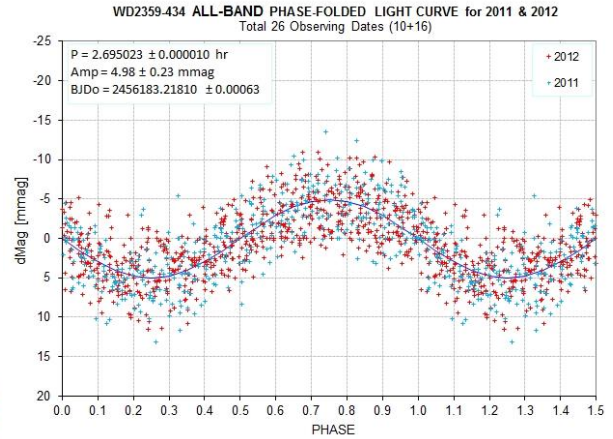


Figure 4. Phase-folded light curve for both 2011 and 2012 observing seasons, allowing solution for all ephemeris parameters.

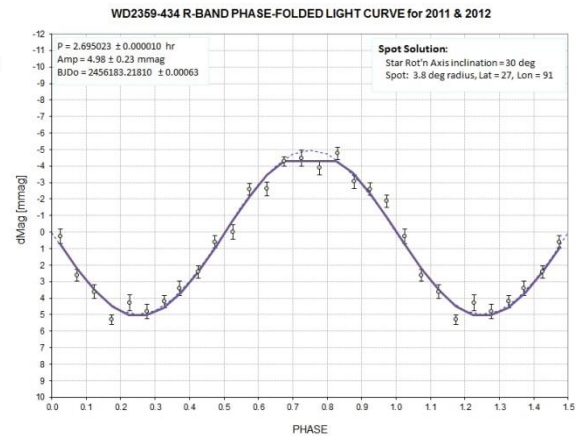


Figure 5. Phase-folded data for 2011 and 2012 observing seasons, binned by phase, with a sinusoidal fit (dashed blue) and starspot fit (solid blue).

5. Interpretation of Phase-Fold Results

Several WDs have been found to pulsate with periods within the range of 0.03 to 0.33 hours (Mukadam *et al*, 2004), and are produced by “non-radial, gravity-waves”. A periodicity of 2.7 hours is well outside the known range of these pulsations, so this cannot be the explanation for WD 2359-434’s variability. WD rotation periods are typically hours to days, so we are justified in identifying the 2.7-hour variability as possibly due to rotation. Variability for cool WDs with weak magnetic fields, like WD 2359-

434, are usually attributed to starspots (Brinkworth *et al*, 2007). That’s the most conservative explanation, treated next.

5a. Starspot Model

A crude one-starspot model was used to fit the phase-folded light curve of Fig. 5. Effective brightness temperatures outside and inside the starspot were adopted to be 8650 and 8150 K; *i.e.* the starspot is assumed to be ~ 500 K cooler than its surroundings. The ratio of blackbody fluxes for these two temperatures = 0.843 at R-band (cf. Fig. 8). A chi-squared solution yields inclination = 30 degrees, starspot latitude = 27 degrees and starspot radius = 3.8 degrees. The starspot solution has a reduced chi-squared = 1.78. A two-starspot model produces essentially the same reduced chi-square, so the one-starspot model is preferred. We propose as one interpretation of the ~ 5 mmag variation this starspot model, shown in Fig. 6.

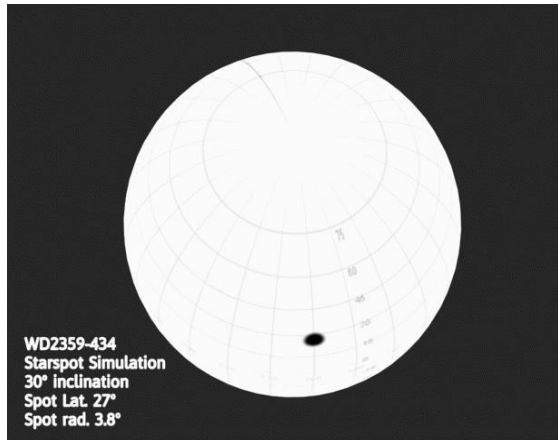


Figure 6. Starspot model that fits the Fig. 5 phase-folded light curve, kindly provided by Manuel Mendez (Spain). This is a view from Earth.

The amplitude difference between 2011 and 2012 can be accommodated by hypothesizing that the starspot changed size from a radius of 4.0 degree to 3.7 degrees during the one year interval. An alternative interpretation is that the effective temperature of the starspot interior increased slightly. For example, the starspot could have undergone a change in temperature from its surroundings from 554 to 466 K during the year interval. Of course, some combination of starspot size and starspot temperature could also account for the change in amplitude.

If a starspot is causing WD 2359-434 brightness to vary then the spot might move in longitude during the 1.1 years of observations. Movement at a constant rate would be observationally indistinguishable from no movement but with a slightly different rotation period, whereas movement with a varying rate would reveal itself in a phase stability plot. Figure 7 is a phase stability plot constructed by adopting the 2011/12 solution for amplitude, BJDo phase and period. For each observing session’s data two parameters were allowed adjustment in order to minimize chi-squared for that light curve: magnitude offset (typically < 1 mmag) and phase offset. In addition, outlier data were identified using chi-squared > 5 as a criterion.

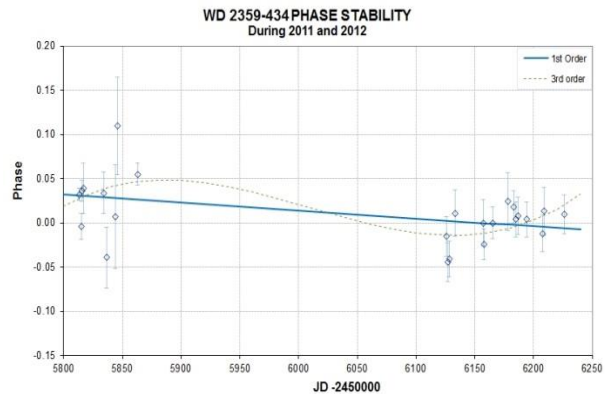


Figure 7. Sinusoidal variation phase versus date for 24 observing dates with linear and 3rd-order fits.

Figure 7 is a plot of the phase adjustments for the 24 observing sessions of 2011/12. Error bars are SE, using phase adjustments that produced chi-squared increases of 1. The straight line fit has a slope that could be removed by merely adopting a slightly adjusted period (from 2.695023 hours to 2.695050 hours). This period is statistically compatible with both the 2012 and 2011/12 periods. The reduced chi-squared value for the straight line fit = 1.49. A third order fit to the data ($y = y_0 + a \times x + b \times x^2 + c \times x^3$) is also shown in Fig. 7; it has reduced chi-squared = 1.16. This improvement is mostly dependent upon three light curves (one at 2455863 and two at ~ 2456127). Because of the limited number of data (N = 24) the 2-sigma range for acceptable reduced chi-squared is 0.51 to 1.66, based on a cumulative distribution function for Gaussian distributions

(Andrae *et al*, 2010). The value 1.49 has a 1.7-sigma statistical significance. The straight line model fit in Fig. 7 is therefore acceptable. The case for phase variability is too weak to be accepted, so we can accept the possibility that WD2359-434’s brightness variability is not changing on a yearly timescale.

Given that there are no significant changes in WD2359-434’s brightness variation amplitude, period or phase during the 2011/12 observing interval we are permitted to consider other explanations, specifically, those that require a fixed amplitude, period and phase. These would include the exoplanet reflected light explanation, which in its simplest geometry produces a nearly perfect sinusoidal variation that should remain fixed for long timescales.

5b. Exoplanet Model

The 4.98 ± 0.23 mmag sinusoidal variation could be produced by an exoplanet in an orbit with an inclination close to 90 degrees, but not so close to 90 degrees that a transit occurs. Adopting a mass for the star of $(0.78 \pm 0.15, 0.05) \times$ solar mass, and a period of 2.695 hrs, the orbital radius for the putative planet would be $0.00419 \pm 0.00026, 0.00009$ a.u. (*i.e.*, 627,000 km). Using a white dwarf mass/radius relation we estimate that WD 2359-434 has a radius of $(0.0103 \pm 0.0019, 0.0026) \times$ solar radius (*i.e.*, 7169 km, or $1.12 \pm 0.21, 0.28 \times$ Earth radius).

This geometry means that the star would appear as having a diameter of $1.31 \pm 0.15, 0.31$ degree viewed from the exoplanet. This corresponds to a solid angle of $(6.53 \pm 1.6, 2.7) \times 10^{-5}$ steradian. This can be equated to the ratio of the surface brightness of the planet to the surface brightness of the star, when the planet is viewed in completely illuminated (“full phase”), assuming an albedo of 100% and orbit inclination close to 90 degrees.

The ratio of the planet’s flux to the star’s flux (for full phase) is the product of the surface brightness and solid angle as viewed from Earth. This allows us to solve for the ratio “radius of the planet / radius of the star.” The peak-to-peak change in brightness is 9.96 ± 0.46 mmag, so the ratio of brightness at the

brightest phase to the faintest phase is 1.0092 ± 0.0004 . In other words, the extra flux at the brightest phase compared with the faintest phase is 0.92 ± 0.04 % of the flux at the faintest phase (when the planet is reflecting negligible light in Earth’s direction). Given this change in the brightness of the “planet plus star” system for “full phase” to “new phase,” the apparent solid angle of the planet would have to be $141 \pm 101, 28$ times the star’s solid angle; the planet’s radius would have to be $11.9 \pm 3.7, 1.3$ times the star’s radius. Assuming the planet had an albedo of 100% it would have to have a radius $1.23 \pm 0.68, 0.41$ times the effective radius of Jupiter (*i.e.*, taking into account Jupiter’s ellipticity). A lower albedo assumption would of course require a larger planet (*e.g.*, 80% albedo requires $R_p = 1.37 \pm 0.76, 0.46 \times R_j$).

6. Amplitude vs. Wavelength

Distinguishing between the starspot and exoplanet interpretations might be helped by knowing how the amplitude of variation depends on wavelength. For example, starspots on cool stars should have a greater amplitude at shorter wavelengths due to the difference in blackbody brightness distribution versus wavelength for the cooler starspot and warmer surroundings.

“Effective wavelength” for a filter depends on not only the filter used, but the CCD QE function, optical component transparency versus wavelength, atmospheric extinction versus wavelength and also the star’s spectral energy distribution (SED). For stars with WD2359-434’s SED, and for typical telescope optics, CCD QE function and atmospheric extinction versus wavelength, the effective wavelengths for each filter are given in Table 3.

Filter	Effective Wavelength
B	441 nm
V	542 nm
Rc	632 nm
Cb	645 nm

Table 3. Effective Wavelength for Filter Bands

Since Rc and Cb filters have nearly the same effective wavelength for this observing situation those data have been combined for the purpose of investigating the dependence of amplitude on wavelength (in Fig. 9).

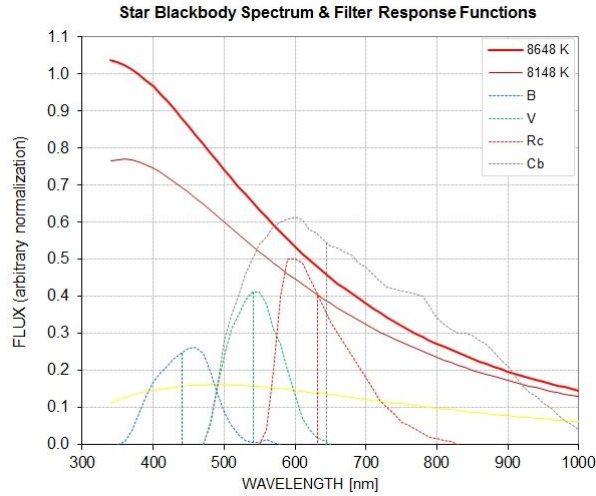


Figure 8. Spectral energy distribution (SED), energy flux per unit wavelength interval, for WD2359-434 (thick red) and for the interior of a possible starspot (thin brown). Filter response referred to outside the atmosphere is also shown for a star with WD2359-434's SED and four filters. A blackbody spectrum for the sun's temperature is shown by the yellow trace. (Filter Cb is a blue blocking filter, with a long pass transition at ~ 490 nm.) Effective wavelengths are shown by the vertical lines.

During the 2011 and 2012 observing seasons 16 and 28 light curves were produced. Some were too short for an accurate determination of amplitude, and the noise level for each varied. A scheme for calculating weights for each light curve was devised (observing session length / RMS internal noise), and this was used to group data into poor quality, medium quality and good quality. The medium and good quality amplitudes are plotted versus wavelength in Fig. 9.

The amplitude of variation at B-band and R-band are statistically the same: B-band amplitude = 4.96 ± 0.49 mmag, $N = 6$, and R-band amplitude = 4.47 ± 0.18 , $N = 11$. The difference is B-band amplitude minus R-band amplitude = $+0.49 \pm 0.52$ mmag (1-sigma significance). Therefore there is no statistically significant dependence of amplitude with wavelength across the optical spectral region.

The “Starspot -500” trace in Fig. 9 is based on a starspot model in which the starspot brightness temperature is 8148 K while the rest of the star surface is at 8648 K. A vertical adjustment was achieved by changing a parameter related to starspot area. Starspot area and temperature difference have similar effects on amplitude, so this particular amplitude fit is merely a solution for “spot area \times temperature difference.” Using this solution the predicted amplitude ratio for B- and R-bands is 1.34. The observed ratio is 1.11 ± 0.27 . Therefore the observed ratio of variation amplitude is compatible with the starspot model; it is also compatible with there being no dependence upon wavelength.

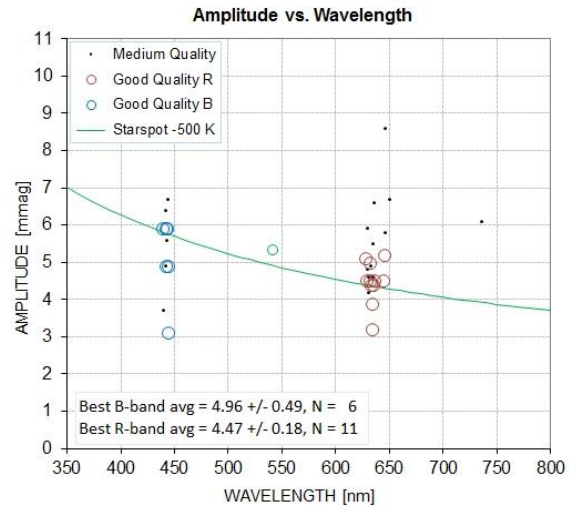


Figure 9. Amplitude versus wavelength for the “medium” and “good” quality data. The “Starspot -500” trace is for a starspot 500 K cooler than its surroundings with vertical adjustment for best fit with observations, e.g., starspot radius = 3.8 degrees. Wavelengths have been “fuzzed” using random offsets to make their plotted symbols overlap less.

An exoplanet that reflects starlight can produce a wavelength dependence of amplitude because the planet’s atmosphere can have an albedo that varies with wavelength. An analysis by Marley *et al* (2013) shows that the albedo can be flat with wavelength throughout the B- to R-band region (far enough from star for the presence of thick water clouds), or it could vary greatly, from ~ 60% to 20% (planet closer to star and mostly cloudless). Therefore the present observations cannot be used to rule out an exoplanet explanation for ED2359-434’s brightness variation.

7. Suggested Follow-Up Observations

How feasible would it be to use radial velocity (RV) measurements to distinguish between the alternative interpretations for WD 2359-434's brightness variation? If the planet's mass were twice Jupiter's, for example, it would produce a radial velocity peak-to-peak variation of 2.4 km/s. RV measurements of this WD were reported by Maxted and Marsh (1999). When their eight RV values are phase-folded using the 2.7-hour brightness variation period, as shown in Fig. 10, there is no discernible sinusoidal signal (it is unfortunate that the data cluster around one phase). However, the uncertainty of each measurement is ~ 4 km/s, so these data are not accurate enough to show the expected variation. The measurements were made with the 3.9-meter Anglo-Australian Telescope at Siding Spring, Australia. The desired accuracy might be achieved by either more measurements with an equivalent telescope and spectrograph or measurements with a more capable system. This may be the only way to determine if the WD 2359-434 brightness variations are caused by a starspot or an exoplanet.

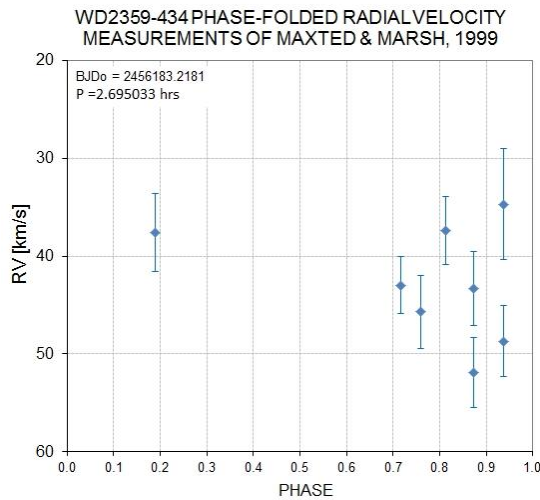


Figure 10. Maxted and Marsh (1999) radial velocity measurements of 1997 and 1998, phase-folded using the ephemeris determined by 2011 and 2012 brightness temperature variations.

One complication with interpreting RV measurements when a starspot is present is that fitted line wavelength will change as the starspot rotates from the approaching side to the receding side of the

planet. However, this effect also causes line shape to change, and the starspot influence on RV plots can be removed, as shown by Moulds *et al* (2013).

Another follow-up observation is suggested by Bergeron (2012), who wonders if convective activity is causing a transformation from spectral type DA to DB, with variability produced by a patch of helium on the surface. This situation should be detectable using spectroscopic observations.

A “hot Jupiter” exoplanet might be detectable from its atmospheric Lyman- α emission, as suggested by McCullough (2013) and Menager *et al* (2011). If it is present then a spectroscopic radial velocity signal might reveal a 2.7-hour period with a greater velocity range than is produced by the WD due to the planet's greater orbital velocity.

As a curiosity let's ask if a planet at the 0.0042 a. u. distance from WD 2359-434 would be within the star's habitable zone? If the planet's albedo were 80% it would be absorbing ~ 5 times as much light per unit area as the Earth absorbs from the sun. Such a planet, and any moons that it might have, would not be within the habitable zone, and it would be too hot for the presence of liquid water. Such a planet could be called a “hot Jupiter.”

8. Conclusions

The case of WD 2359-434 illustrates the feasibility of detecting exoplanet candidates orbiting white dwarfs using the planet's reflected light (using amateur telescopes). Whereas an exoplanet system like the one hypothesized for WD 2359-434 would exhibit transits for only 4.5 % of random orbit inclinations, the reflected light geometry permits detection for ~ 50 % of random orientations. This ten-fold advantage suggests that precision photometry measurements of brightness variations, having periods of several hours, might be a more productive strategy for detecting Jupiter-size exoplanet candidates orbiting white dwarfs than the alternative strategy of searching for exoplanet transits. Follow-up verification using RV measurements will be required to distinguish between the starspot and exoplanet interpretations, and this

may be the greater observing challenge. However, before RV follow-up observations can be justified it may be necessary to monitor the white dwarf's brightness variability for more than a year in order to assess constancy of period, amplitude and phase, because any changes in these parameters would rule out the exoplanet interpretation and favor a starspot interpretation.

9. Acknowledgements

Appreciation is expressed to Eric Agol for 1) inspiring the PAWM project (that led to discovering that WD 2359-434 was variable), 2) helping recruit observers for PAWM, and 3) independently deriving an exoplanet size for a preliminary set of sinusoidal amplitude and star properties data, allowing approximate confirmation of the procedure used in this paper. We want to thank the 38 observers, mostly amateur, who contributed observations for PAWM; the variability of WD 2359-434 would not have been discovered without this group effort. Thanks to Manuel Mendez for graciously creating images and animations of a white dwarf with starspots, one of which is used in this publication. One of the authors (AF) would like to acknowledge the Microlensing Applications in Astrophysics (MOA) collaboration to permit WD2349-434 observations, and to also thank the University of Canterbury for allowing MOA to use the B&C telescope. We acknowledge brief reviews of this manuscript by Dr. Luca Fossati and Dr. Peter McCullough, and the latter's suggestion for Lyman- α follow-up observations.

10. References

- Agol, E., 2011, *ApJL* **731**, L31.
- Agol, E., Relles, H., 2012, private communication.
- Andrae, R., Schulz-Hartung, T., Melchior, P., 2010, <http://arxiv.org/abs/1012.3754>.
- Bergeron, P., Saffer, R. A., Liebert, J., 1992, *ApJ* **394**, 228.
- Bergeron, Pierre, 2012, private communication.
- Brinkworth, C. S., Burleigh, M. R., Marsh, T. R., 2007, 15th European Workshop on White Dwarfs, ASP Conference Series, Vol. 372, R. Napiwotzki and M. R. Burleigh.
- Cuadrado, A. *et al*, 2004, *A & A* **423**, 1081–1094.
- Dobbie, P. D., Burleigh, M. R., Levan, A. J., Barstow, M. A., Napiwotzki, R., Holberg, J. B., Hubeny I., Howell, S. B. , 2005, *MNRAS* **357**, 1049-1058.
- Fossati, L., Bagnulo, S., Haswell, C. A., Patel, M. R., Busuttil, R., Kowalski, P.M., Shulyak, D. V., Sterzik, M. F., 2012, *Astrophys. J. Lett.* **757**, 1, L15-21.
- Holberg, J. B., Sion, E. M., Oswalt, T., McCook, G. P., Foran, S., Subasavage, J. P., *AJ* **135**, 1225.
- Lajoie, C. P., Bergeron, P., 2007, *ApJ* **667**, 1126-1138.
- Marley, Mark S., Ackerman, Andrew S., Cuzzi, Jeffry N., Kitzmann, Daniel , 2013, arXiv: 1301.5627v1.
- Maxted, P.F.L., Marsh, T.R., 1999, *Mon. Not. R. Astron. Soc.* **307**, 122.
- McCullough, Peter, 2013, private communication.
- Menager, H., Barthelemy, M., Koskinen, T., Lilenstein, J., 2011, *EPSC Abstracts*, Vol. 6, EPSC-DPS2011-581-1.
- Moulds, V. E., Watson, C. A., Bonfils, X., Littlefair, S. P., Simpson, E. K., 2013, (submitted to MNRAS), arXiv:1212.5922v2.
- Mukadam, Anjun S. *et al*, 2004, *ApJ* 607, pp 982-998.
- Napiwotzki, R. *et al*, 2003, *ESO-Messenger*, **112**, 25.
- Sion, Edward M., Holberg, J. B., Oswalt, Terry D., McCook, George P. , Wasatonic, Richard, 2009, *AJ* **138**, 1681.